Retardation-induced plasmonic blinking in coupled nanoparticles

Holger Fischer* and Olivier J. F. Martin

Nanophotonics and Metrology Laboratory, Swiss Federal Institute of Technology (EPFL), Lausanne, Switzerland
**Corresponding author: holger.fischer@epfl.ch*

Received September 23, 2008; revised December 10, 2008; accepted December 15, 2008;
posted January 6, 2009 (Doc. ID 101677); published January 30, 2009

We study how retardation leads to interference effects in radiatively coupled plasmonic nanoparticles. We show that inclined illumination through a glass substrate on two plasmonic particles results in either an enhanced field or an attenuated field localized at the position of the first particle. Periodic intensity blinking of the first particle is observed as a function of the particle separation. This phenomenon is nonsymmetric, and almost no blinking is observed on the second particle. The effect is strongest when the illumination angle is chosen such that the optical retardation path in the substrate coincides with the particle distance. Implications of this plasmonic blinking for near-field measurements are discussed. © 2009 Optical Society of America

OCIS codes: 260.3910, 050.6624, 240.6680.

The properties of coupled plasmonic particles have been studied intensively in the past few years in the context of nanoscopic waveguiding [1,2], hotspot engineering [3–7], and plasmonic biosensing [8,9]. In most cases the size of the particles and the particle separation distance are small enough that the quasistatic approximation is valid. However, even at these dimensions, retardation can play a role [10]. Furthermore, when retardation effects augment, additional modes can be excited that are not observable in the nonretarded case [11]. It has also been demonstrated that periodic near-field coupled particle chains or arrays support asymmetric near-field distributions caused by retardation [12,13]. Furthermore, experimental and numerical investigations of the plasmon line shape reveal extremely narrow resonances for far-field coupled plasmonic nanoparticle chains [14–17]. These last studies however concentrate on the spectral character of the entire coupled system in a homogeneous background medium.

In this Letter we study the near field of two far-field coupled plasmonic particles. We evidence the central role of relative phase retardation between the particles. The implications of the observed phenomena for experimental measurements are also discussed.

The Green's tensor method is used to calculate the near-field intensity of a coupled plasmonic particle pair [18–20]. The experimental data of Johnson and Christy are used as a dielectric function for gold [21]. The plasmonic particles with the dimensions 40 nm $\times$40 nm$\times$80 nm are placed on a substrate with index $n_s=1.5$ or $n_s=2.0$; see Fig. 1. The structure is then illuminated from below through the substrate. The incident field is polarized parallel to the long axis of the particles. The relative field intensity at the edge of each particle and at the plasmon resonance ($\lambda=635$ nm for $n_s=1.5$ and $\lambda=700$ nm for $n_s=2.0$) of each individual particle is calculated as a function of the particle separation d. The illumination is inclined by the angle α with respect to the vertical axis, such that the **k** vector of the incident light is perpendicular to the long axis of the plasmonic particles (Fig. 1).

Figure 2 shows the field intensity at the edge of particle 1 and of particle 2 as a function of the particle separation d and the illumination angle α. Two observations can be made immediately from Fig. 2. First, the intensity on both particles increases for inclined illumination, compared to normal incidence ($\alpha=0°$), with a sharp maximum at $\alpha=42°$. Second, strong intensity oscillations are observed in particle 1 as a function of the particle separation for all $\alpha>0°$, with a maximum oscillation amplitude at $\alpha=42°$. At this illumination angle the oscillation period is 320 nm, which is half the incident wavelength. The field intensity of particle 2 is not subject to such strong oscillations, which leads to configurations where the field maximum of the structure is either located at particle 1 or at particle 2, depending on the particle separation distance d.

This phenomenon can be explained considering the radiative coupling of the particles. In fact, for a substrate index $n_s=1.5$, at $\alpha=42°$ the optical path length of the retardation distance r coincides with the particle separation d. Note that this phenomenon occurs when α fulfills the total internal reflection condition,

$$1/n_s = \sin(\alpha). \tag{1}$$

The scattered radiation of particle 1 at the position of particle 2 has thus for all separation distances d a

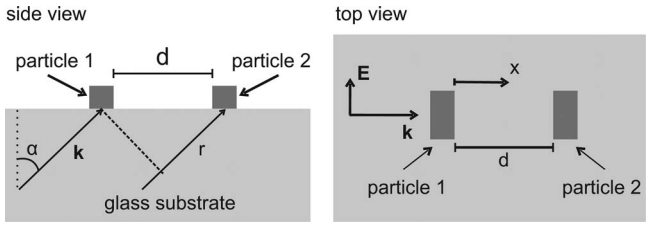

Fig. 1. Particles are illuminated through the glass substrate at an angle α. The resulting retardation distance r and the particle separation distance d are indicated in the figure.

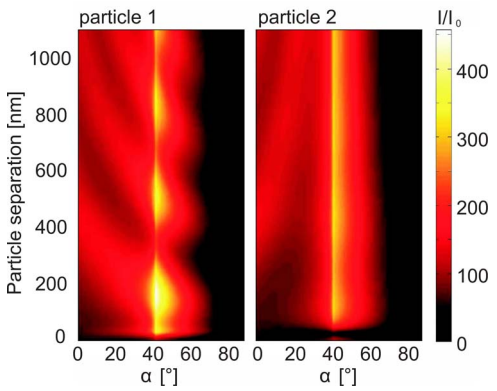

Fig. 2. (Color online) Relative field intensity at the edges of particle 1 and of particle 2 plotted as a function of the incident angle α and of the particle distance d at the plasmon resonance $\lambda = 635$ nm for $n_s = 1.5$. The intensity of particle 1 is subject to strong oscillations as a function of the particle separation for all incident angles. The strongest field and the strongest oscillation contrast are observed at $\alpha = 42°$, where the optical path length of the retardation distance r coincides with the distance d of the particles.

constant phase difference to the direct excitation of particle 2. Hence, the phase difference between the scattered radiation of particle 2 at the position of particle 1 and the excitation of particle 1 depends on the particle separation. Therefore, the direct excitation field and the light scattered from particle 1 are changing at the position of particle 2 from out of phase for $d = 2n\lambda/4$ $(n = 1, 2, 3, 4, \ldots)$ to in phase for $d = (2n-1)\lambda/4$ $(n = 1, 2, 3, 4, \ldots)$. The resulting destructive and constructive interference leads to the observed intensity oscillations with a period $\lambda/2$.

The same phenomenon is observed when calculations are performed for a substrate of index $n_s = 2$. The angle defined by Eq. (1) is now exactly $\alpha = 30°$. This situation is investigated in Fig. 3(a), where the dashed curve shows the intensity at particle 1 as a function of the particle separation. The strong intensity oscillations are clearly visible. Figure 3(b) shows the phase as a function of the separation distance at the edge of particle 1. The phases of the scattered light from particle 2 and of the illumination are calculated individually. At the particle separation distances where intensity maxima on particle 1 are observed [indicated with the dotted lines in Figs. 3(a) and 3(b)], the scattered radiation of particle 2 is in phase with the direct illumination of particle 1. At the separation distances where intensity minima are observed, the phase difference between the direct illumination of particle 1 and the scattered radiation from particle 2 is π.

Figure 2 also indicates that the oscillation period increases for decreasing α. The interference conditions can still be fulfilled, but for smaller angles α the retardation distance r becomes shorter and thus the period between constructive and destructive interference increases. However, the strongest interference contrast is obtained at $\alpha = 42°$ for a substrate index $n_s = 1.5$ (Fig. 2) and at $\alpha = 30°$ for a substrate index $n_s = 2$ (not shown).

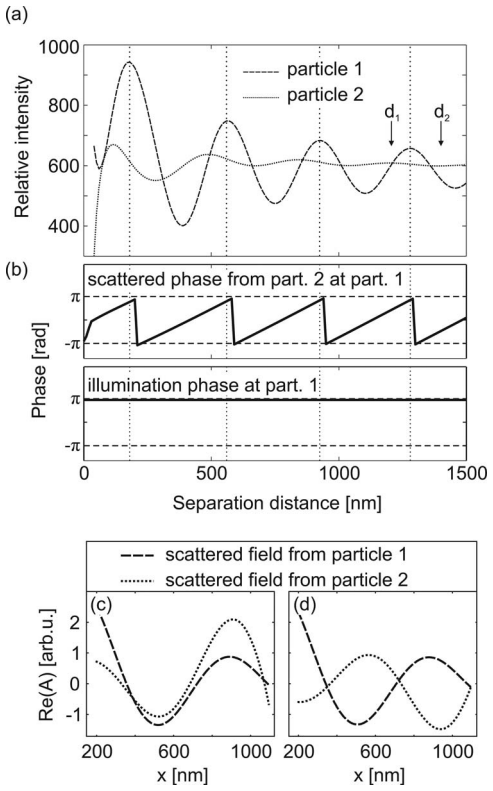

Fig. 3. (a) Field intensity at particle 1 (dashed curve) and at particle 2 (dotted curve) for $n_s = 2$ and $\alpha = 30°$ at the plasmon resonance $\lambda = 700$ nm. (b) Phase of the scattered field from particle 2 and of the illumination field, at the position of particle 1 as a function of the separation distance. At the distances where intensity maxima are observed in (a), the phases of the scattered field from particle 2 and the phase of the direct illumination coincide. (c), (d) x components of the real part of the scattered complex amplitude A between both particles at the particle separation distance $d_1 = 1200$ nm and $d_2 = 1400$ nm, respectively. The two counterpropagating waves are in phase at the intensity maxima in particle 2 and out of phase at the intensity minima in particle 2.

The dotted curve in Fig. 3(a) shows that particle 2 is also subject to intensity oscillations, however, with a much weaker amplitude than that observed on particle 1. Since the phase difference between the scattered light from particle 1 and the direct illumination at particle 2 is constant for all particle separations, the oscillations observed at particle 2 must have a different origin from those observed at particle 1. Figures 3(c) and 3(d) show the x components of the real part of the scattered complex amplitude A from particle 1 (dotted curve) and particle 2 (dashed curve) between the two particles for a particle separation $d_1 = 1200$ nm and $d_2 = 1400$ nm, respectively. At the particle separation $d_1 = 1200$ nm the intensity on particle 2 is maximal and the two counterpropagating waves in Fig 3(c) are in phase. At the particle separation $d_2 = 1400$ nm the intensity on particle 2 is minimal and the two counterpropagating waves in Fig. 3(d) are out of phase. The intensity oscillations at particle 2 are thus due to Fabry–Perot-like resonances between the two plasmonic particles. An impact of these resonances on the intensity of particle 1 cannot

be observed, since the blinking effect discussed previously is much stronger than the Fabry–Perot effect and dominates the intensity oscillations at particle 1.

Obviously, the oscillation amplitude of the plasmonic blinking decreases for increasing particle separation. However, Fig. 4(a) demonstrates that the phenomenon can still be observed even for large particle separations of several times the resonance wavelength $\lambda = 700$ nm. The relative intensity is plotted as a function of the particle separation for a substrate with $n_s = 2$ and with $\alpha = 30°$.

This coherent radiative interaction of nanoparticles at large distances is extremely important for experimental studies of plasmon resonant nanoparticles: Even with a particle separation of several micrometers, the radiative coupling between the particles can still lead to strong particle interactions that may modify the particle near field significantly. This effect can be particularly important for photon scanning tunneling microscopy, where the near-field probe can act in such an experiment as a second nanoparticle. Hence radiative probe–sample interaction can significantly influence the measured near field.

Note that the observed blinking phenomena are not limited to *plasmonic* nanostructures but can also be observed for dielectric particles. However, in that case the modulation is extremely weak.

In conclusion, retardation effects in radiatively coupled plasmonic nanoparticles have been studied numerically. The substrate index defines the illumination angle where the optical retardation path coincides with the particle separation. At this angle, the field intensity around the nanoparticles is maximized owing to the interference of the direct illumination and the scattered light from the particles. Furthermore, the interference of the direct illumination and the scattered light leads to asymmetric plasmonic blinking as a function of the particle separation. The radiative coupling decays with increasing particle separation, but remains rather strong, even for relatively large distances. The implications of this effect for near-field measurements—even of single particles—have been discussed.

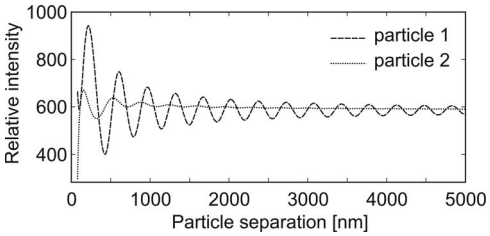

Fig. 4. Relative field intensity at particle 1 (dashed curve) and at particle 2 (dotted curve) as a function of the particle separation at the plasmon resonance ($\lambda = 700$ nm) and $\alpha = 30°$.

Funding from the Swiss National Center of Competence in Research Nanoscale Science is gratefully acknowledged.

References

1. S. A. Maier, P. G. Kik, H. A. Atwater, S. Meltzer, E. Harel, B. E. Koel, and A. A. G. Requicha, Nature Mater. **2**, 229 (2003).
2. C. Girard and R. Quidant, Opt. Express **12**, 6141 (2004).
3. W. Rechberger, A. Hohenau, A. Leitner, J. R. Krenn, B. Lamprecht, and F. R. Aussenegg, Opt. Commun. **220**, 137 (2003).
4. K. Li, M. I. Stockman, and D. J. Bergman, Phys. Rev. Lett. **91**, 227402 (2003).
5. D. P. Fromm, A. Sundaramurthy, P. J. Schuck, G. Kino, and W. E. Moerner, Nano Lett. **4**, 957 (2004).
6. P. Muhlschlegel, H. J. Eisler, O. J. F. Martin, B. Hecht, and D. W. Pohl, Science **308**, 1607 (2005).
7. P. Ghenuche, R. Quidant, and G. Badenes, Opt. Lett. **30**, 1882 (2005).
8. S. Enoch, R. Quidant, and G. Badenes, Opt. Express **12**, 3422 (2004).
9. S. Zou and G. C. Schatz, J. Chem. Phys. **121**, 12,606 (2004).
10. J. P. Kottmann and O. J. F. Martin, Opt. Lett. **26**, 1096 (2001).
11. A. Christ, O. J. F. Martin, Y. Ekinci, N. A. Gippius, and S. G. Tikhodeev, Nano Lett. **8**, 2171 (2008).
12. R. deWaele, A. F. Koenderink, and A. Polman, Nano Lett. **7**, 2004 (2007).
13. A. F. Koenderink, J. V. Hernández, F. Robicheaux, L. D. Noordam, and A. Polman, Nano Lett. **7**, 745 (2007).
14. S. Zou, N. Janel, and G. C. Schatz, J. Chem. Phys. **120**, 10,871 (2004).
15. V. A. Markel, J. Chem. Phys. **122**, 097101 (2005).
16. S. Zou and G. C. Schatz, J. Chem. Phys. **122**, 097102 (2005).
17. A. O. Pinchuk and G. C. Schatz, Mater. Sci. Eng., B **149**, 251 (2007).
18. O. J. F. Martin and N. B. Piller, Phys. Rev. E **58**, 3909 (1998).
19. M. Paulus, P. Gay-Balmaz, and O. J. F. Martin, Phys. Rev. E **62**, 5797 (2000).
20. M. Paulus and O. J. F. Martin, Opt. Quantum Electron. **33**, 315 (2001).
21. P. B. Johnson and R. W. Christy, Phys. Rev. B **6**, 4370 (1972).